Conformational and nuclear dynamics effects in molecular Auger spectra: Fluorine core hole decay in CF_4

T Arion[1]‡, O Takahashi[2], R Püttner[3], V Ulrich[1], S Barth[1], T Lischke[1,4], A M Bradshaw[1,4], M Förstel[5], U Hergenhahn[5]

[1]Max-Planck-Institut für Plasmaphysik, EURATOM Association, Boltzmannstr. 2, 85748 Garching, Germany

[2]Institute for Sustainable Sciences and Development, Hiroshima University, Kagamiyama, Higashi-Hiroshima, 739-8526, Japan

[3]Institut für Experimentalphysik, Freie Universität Berlin, Arnimallee 14, 14195 Berlin-Dahlem, Germany

[4]Fritz-Haber-Institut der Max-Planck-Gesellschaft, Faradayweg 4-6, 14195 Berlin, Germany

[5]Max-Planck-Institut für Plasmaphysik, EURATOM Association, Wendelsteinstr. 1, 17491 Greifswald, Germany

E-mail: uwe.hergenhahn@ipp.mpg.de

Abstract. In a molecular Auger spectrum information on the decaying state is implicitly ensemble-averaged. For a repulsive core-ionized state, for example, contributions from all parts of its potential curve are superimposed in the Auger spectrum. Using carbon tetrafluoride (CF_4, tetrafluoromethane), we demonstrate for the first time that these contributions can be disentangled by recording photoelectron-Auger electron coincidence spectra with high energy resolution. For the F K-VV spectrum of CF_4, there are significant differences in the Auger decay at different intermediate state (single core hole) geometries. With the help of calculations, we show that these differences result primarily from zero-point-fluctuations in the neutral molecular ground state, but are amplified by the nuclear dynamics during Auger decay.

PACS numbers: 07.81.+a, 07.85.Qe, 32.80.Hd, 33.80.Eh

‡ Present address: Institut für Experimentalphysik, Universität Hamburg, Luruper Chaussee 149, 22761 Hamburg, Germany

1. Introduction

Molecular Auger electron spectra initiated by photoionization or electron impact contain contributions from molecules at different geometries, and, sometimes, in different electronic states. The former is a reflection of the neutral ground state population, excited into the singly ionized intermediate state by a sudden process. The temporal evolution of the intermediate state may also leave fingerprints in the Auger spectrum. Best known among these effects is lifetime vibrational interference (LVI), which leads to a redistribution of intensities among vibrational levels of an Auger final state, compared to a static reference system. Generally, both conformational and dynamic effects (LVI) can be treated in a theoretical description of molecular Auger spectra [1, 2] as long as an approach based on Franck-Condon factors is sufficient [3, 4]. This strategy will break down however, when repulsive states come into play, and when the decay amplitudes depend explicitly on the molecular conformation. Both factors might gain in importance when Auger decay of molecules in a chemical environment is considered, as shown in a recent study of liquid water [5].

In this article, we demonstrate experimentally the impact of ground state conformational distributions and of nuclear dynamics in the Auger decay of a repulsive, molecular core ionized state, namely a F $1s$ core hole in CF_4. In our experiment, the exact energy of the intermediate state for every Auger electron was observed by photoelectron-Auger electron coincidence spectroscopy with high energy resolution, as developed by some of the present authors [6, 7, 8] and by others [9, 10]. At fixed photon energy, our measurements show a dependence of the Auger spectrum on the exact kinetic energy of the emitted photoelectron. These results are compared with *ab initio* calculations of the spectra for an ensemble of molecular states, which include a nuclear coordinate dependence of the electronic decay matrix elements.

CF_4 (carbon tetrafluoride, tetrafluoromethane) is a tetrahedral molecule in its ground state. It is chemically inert due to the strength of the C-F bonds. Photoionization of a fluorine K-shell electron, with a vertical ionization energy of $E_b = 695.37(10)$ eV [11], leads to a single, broad and unstructured photoelectron line of approx. 1.5 eV width, as remeasured in our experiment. The width is caused by the dissociative character of the $CF_4{}^+$ F$(1s^{-1})$ state. Strictly speaking, the four fluorine atoms in the molecule are chemically equivalent, and its F $1s$ core ionization leads to a vibronic coupling problem. An important consequence of vibronic coupling in inner shell ionization is the appearance of Born-Oppenheimer forbidden vibrational modes [12, 13]. Often however, these modes can also be introduced by *a priori* localizing the core hole. This latter approach will be used here. In computational studies [14, 15], the separation of a neutral F* containing the core vacancy from the core-ionized molecule was found to be energetically most favourable; at the same time the remaining $CF_3{}^+$ fragment becomes planar. The potential surfaces along this 'umbrella' mode were found to be repulsive.

The F K-VV Auger spectrum of CF_4 has been investigated experimentally [16, 11]

and theoretically [17, 11, 18]. In [17] a semi-empirical description as a self-convolution of the CF_4 valence band structure was given. In the two later papers [11, 18], the authors calculated the energies of the doubly charged states and then assigned Auger amplitudes to them. We will return to these results below. Complementary experiments have been performed with coincidence spectroscopy of two valence electrons [19] and double charge transfer [11]. The resonant Auger decay (autoionization of neutral, core-excited state) of CF_4 has also been investigated, both after C 1s and F 1s excitation [20, 21, 22]. In both cases, the spectra show features that can be attributed to electronic decay of fragments after a fluorine atom has dissociated. Most interestingly in the context of this work, for F 1s-to-antibonding excitation, a part of the decay spectrum results from atomic Auger decay of fluorine, which has acquired a substantial amount of momentum by dissociation [21, 23].

2. Experimental and theoretical methods

Details of our set-up and analysis procedures have been described elsewhere [6, 7]; we therefore refer here only to the details important for this experiment. The measurements were carried out at the UE52/SGM beamline of the BESSY II synchrotron radiation source at the Helmholtz-Zentrum Berlin. Vertically linearly polarized radiation of 706 eV energy and a bandpass of 350 meV was used. We used a combination of a commercial hemispherical electron spectrometer (Scienta ES200) with a set of five linear electron time-of-flight (TOF) analysers to detect two electrons from sequential photo-double-ionization (photoionization followed by Auger decay) in coincidence. The hemispherical analyser operated at a pass energy of 300 eV to record a large portion of the fluorine Auger spectrum at fixed analyser voltages. Energy resolution for the Auger electrons amounted to 580 meV, due to the high pass energy. The photoelectrons of around 10 eV kinetic energy were detected in the TOF analysers. The analyser contribution to the photoelectron energy resolution, for electrons detected in coincidence, was at most 160 meV. In 36 h of multi-bunch acquisition time, about 70000 true photoelectron-Auger electron coincidences were recorded. Data were recorded in list mode, and coincidences were reconstructed by off-line analysis of the data stream.

The sum of all non-coincident Auger spectra, recorded simultaneously, is shown in panel a) of figure 1. The peak structure of this spectrum agrees with earlier data [11]. In the following we shall discuss the time resolution of the coincidence events, which is responsible for the energy resolution of the TOF analysers. The remaining panels of the figure show details of the operation of the hemispherical analyser. Below the spectrum, in panel b), the relation between Auger electron energy and arrival time of the Auger electron on the detector is shown for a small part of the non-coincident data set. As the absolute time-of-flight through the hemisphere, t_{au}, cannot be measured, the zero of the vertical time axis is arbitrary. Somewhat contrary to intuition, electrons with higher kinetic energy have a *longer* transit time through the hemispheres. This is a property of the Kepler orbits on which the electrons travel [24]. The ripple structure

in panel b) results from the multibunch filling of the synchrotron radiation ring. Each ripple pertains to one bunch of the fill pattern, which are spaced by 2 ns. In our data acquisition scheme, arrival times in the TOF analysers are referred to the arrival time of the Auger electron. The time-of-flight broadening in the hemisphere is therefore relevant for the coincident energy resolution (see discussion in [7] and [25]). Here we show that under conditions of this experiment, the time broadening is much lower than in studies with lower pass energy referred to above. This explains the good energy resolution for the photoelectrons. In perspective, it would even be possible to recover the full time-of-flight resolution accessible when BESSY is operating in the single bunch mode, by compensating for the time broadening in the data analysis (see data in panel (c)). This point was also discussed by other authors [26]. The functional dependence of the transition time through the hemispheres on Auger kinetic energy, seen as the slope of the ripples in the ε_{au} vs. t_{au} map, is corrected for in the data analysis [7, 25].

Calculations of the temporal dynamics of the Auger decay spectrum of CF_4 are reported here for the first time. We aim at simulating conformational effects on the Auger spectrum by combining molecular dynamics (MD) simulations with calculations of the Auger decay matrix elements. Ground state MD trajectory calculations using zero-point vibrational energies were performed to sample the initial state geometry. The time step was set to 1.0 fs and the system was propagated 10000 times. One hundred points in the snapshots thus obtained were sampled randomly. This cycle was performed five times: thus in total five hundred initial geometries were sampled. In order to explore the dynamical effect in the excited state, core-ionized MD simulations were propagated for 10 fs with a time step of 0.1 fs. For each geometry, the Auger decay spectra were calculated.

The detailed computational procedure used for calculating the Auger decay spectra has been described [27, 28]. Briefly, a set of ground state molecular orbitals (MOs) was obtained by standard SCF calculations. In the normal Auger transition, the final state wave functions contain $(N-2)$ electrons with possible singlet and triplet spin multiplicities. Limited spin-symmetry-adapted CI calculations within the two-hole valence space were performed to determine the Auger final state wave functions. The Auger transition probability is approximated simply by atomic populations of valence orbitals on the excited atom while neglecting the term associated with the Auger electron itself. The Auger decay calculations were performed for each dynamics calculation snapshot. The theoretical spectra were constructed by convolution of the line spectra using Gaussian functions with a fixed full width at half maximum of 1.0 eV. The final spectra were obtained by summation of spectra at 0.1 fs time steps from a series of trajectories weighted by the lifetime decay ratio $\exp(-t/\tau)$, where τ is the lifetime of the core hole of 2.0 fs [29].

3. Results

The photoabsorption spectrum of CF_4 at the fluorine K-edge is characterized by a below threshold resonance corresponding to an excitation into the $5t_2$ anti-bonding orbital [30]. The cross-section above the ionization edge is almost structureless. An absolute photabsorption cross-section measurement [31] at good signal-to-noise ratio shows two weak above-threshold resonances in the 700 to 750 eV range (figure 2) [32], in agreement with earlier work [33]. Both correspond to modulations in the cross section of 6 % or less. The first resonance can be identified in measurements of the total ion yield [34], but partial yield data are not of sufficient quality to give insight into its nature. The measurements of the Auger spectrum presented in this paper have been carried out at $h\nu = 706$ eV to benefit from the high photoionization cross section, and a low kinetic energy of the photoelectrons, which makes it easier to obtain a good energy resolution in the TOF analyzers.

In our co-incidence experiment, it is possible to differentiate between F *K-VV* Auger spectra pertaining to different kinetic energies of the photoelectrons forming the broad, unstructured F 1*s* line. Figure 3 clearly shows that different Auger final states have a propensity to become populated from different parts of the photoelectron line. This constitutes the main experimental result of the present paper.

The structure of the electron-electron coincidence spectrum in the $\varepsilon_{ph}, \varepsilon_{au}$ plane, as shown in panel a) of figure 3, gives information on the potential energy curves of the states involved. For bound-to-metastable transitions as observed in small molecules, such as CO, the Franck-Condon factors can lead to a variety of complex structures in this plane [4, 6, 7]. In methane, representing the case of a transition from a bound intermediate to a set of unbound final states, the coincident spectrum appears mostly to be arranged along the lines of constant intermediate state energy [8]; these lines correspond to the $v' = 0$ and $v' = 1$ core ionized states and would be horizontal in the present figure. On the other hand, the present coincidence spectrum of CF_4 is mostly structured along vertical lines, *i.e.* lines of constant Auger energy. Transitions grouped along these lines in the coincident data plane can arise, if the potential curves of the core-hole involved and the dicationic final states are both unbound, and approximately parallel. A feature with diagonal variation (dashed line), as is the case for peak 7 in figure 3, can be explained with a potential energy curve of the dissociative final state that is steeper than that of the unbound core-hole state.

To demonstrate more clearly that different types of dicationic states can be populated from different parts of the intermediate potential curve, we have integrated the coincident Auger spectrum for three different intervals of the photoelectron energy, covering the center of the photoline and the low and high energy flanks, at intensities a factor 0.5 lower than the peak maximum. The resulting spectra are shown in Fig. 4. It is clear that states at low core hole binding energy tend to populate Auger final states with low binding energy more strongly, and vice versa.

4. Discussion

The interpretation of the Auger spectrum has been greatly helped by a population analysis of the two-hole states by previous authors [18]. Gottfried *et al.* found that the observed peaks 1 and 2 can be assigned to states with two holes localized at two different F ligands, one in an F 2*p*-derived σ-bonding orbital and one in a lone pair orbital. We will designate them as $F_1^{-1}F_2^{-1}$. The less strongly bound $F_1^{-1}F_2^{-1}$ states with two lone pair holes are not populated by Auger decay. The more strongly bound peaks 4-7 correspond to both vacancies located at a single fluorine atom (F^{-2}). For this group of states, energy differences are determined by a strong singlet-triplet splitting, rather than by the orbital character. Peak 3 is a blend of the two regimes.

4.1. Inital state effects

None of the theoretical studies mentioned so far has targeted the dependence of the Auger spectrum on nuclear coordinates. We have therefore undertaken new calculations of the F *K-VV* spectrum of CF_4, in which we use molecular dynamics (MD) simulations to take into account the effect of different molecular geometries on the decay. Such effects can be two-fold: A dependence of the ionization energy on the nuclear geometry can become manifest due to zero-point fluctuations around the equilibrium geometry of the ground state. This effect is reminiscent of photoline profiles in clusters, which result from the presence of different isomers in the neutral initial state [35]. Secondly, after core ionization the dynamics of the ionized state evolves, while Auger decay takes place. This can lead to profound differences in the decay spectrum viewed at different decay times [28]. In the present case, the first effect is expected to be dominant because the change in the nuclear geometry within the lifetime of the core-ionized state is less than 0.03 Å along the relevent coordinate (see below).

Results from these calculations are shown in Fig. 5. Here we show the Auger spectra calculated at three different photoelectron energies representing the intervals in Fig. 4. The calculations obviously reproduce the vertical lines for peaks 1 to 6 and the diagonal line for peak 7 found in panel a) of Fig. 3. In particular, they also reproduce the propensity for low binding energy intermediate states to decay into low energy final states.

In order to interpret this finding we have attempted to correlate the calculated photoelectron energy, different for each of the initial state samples, to the geometry of that state (bond lengths and angles). The coordinate bearing the clearest relation to photoelectron energy ε_{ph} is R_{CF^*}, the separation between the carbon center and the core-ionized fluorine atom (with the *a priori* localized core hole). This dependence is shown in Fig. 6. Equipped with this information we are now in a position to explain the present experimental data: $CF_4{}^+$ (F $1s^{-1}$) dissociates into $CF_3{}^+$ and a neutral, core excited F^* atom. On the same time scale it undergoes Auger decay. If the dissociation process were complete before autoionization takes place, the decay would be purely atomic, as seen for some resonant Auger processes (e.g. [36, 37, 21]). However, during

the F 1s core-hole lifetime of around 2 fs the C-F* distance elongates by only 0.02-0.03 Å, *i.e.* 10 % of the variation caused by the zero-point vibration. Due to the ground state fluctuations, in some states this dynamics will start out with a C-F* bond that is already elongated with respect to the ground state, giving rise to the high energy flank of the photoelectron peak. We expect that local, atomic decay amplitudes in states with a long C-F* bond will play a more important role than for the rest of the spectrum. In Figs. 4 and 5 it is indeed found that they have a propensity to decay into $F_1^{-1}F_2^{-1}$ final states. Here, the lone pair vacancy is produced by a quasi-atomic decay of the F*, and the second vacancy, in a bonding orbital of the $CF_3{}^+$ fragment, is created by polarization effects which draw charge towards the F* atom already before the decay. All of that said we note that dissociation into $CF_3{}^+$ and F* in our interpretation is the dominating, but possibly not the only pathway for the core-excited molecule. Evidence for alternative channels will be discussed below.

4.2. Nuclear dynamics during Auger decay

The temporal dynamics further fosters atomic-like decays, as seen in figure 7. The more time that passes between photoionization and Auger decay, the more molecules end up in $F_1^{-1}F_2^{-1}$ final states, in which the holes are localized at two different fluorine atoms. Effects are notable within the lifetime of the core hole (2 fs), and become very pronounced at even longer times. As the majority of holes decays earlier, the overall contribution to the observed spectrum is, however, limited. This finding is in agreement with observations in resonant Auger decay of CF_4 [20, 21, 22]. A simplified, pictorial representation of the main ideas given above is shown in figure 8.

We have so far ignored non-local autoionization amplitudes, known as ICD (Interatomic Coulombic Decay) or ETMD (Electron Transfer Mediated Decay) [38]. These channels can be important in molecular Auger decay, as indicated by calculations for the Xe fluorides [39], and in an experiment on SiF_4 [40]. If we stick to the picture of a decaying F* atom in the vicinity of a $CF_3{}^+$ ionic fragment, ICD-like decay amplitudes would lead into F + $CF_3{}^{2+}$ final states, which would explain that even for the most asymmetric configurations about half of the intensity is in such final states. An in-depth discussion of this topic has to await more detailed calculations.

Figure 9 shows the full calculated Auger spectrum for decays that occur 10 fs after the photoionization process. This spectrum represents the asymptotical limit of the time evolution. It is assumed that at that time the dissociating fragments CF_3 and F are separated sufficiently to consider the Auger decay of the F 1s core hole as an atomic process. Generally, we therefore expect an Auger spectrum that very roughly divides into three groups, pertaining to $2p^{-2}, 2p^{-1}2s^{-1}$ and $2s^{-2}$ final states. This expectation is borne by the figure, however every group appears to be sub-divided into several peaks. The latter can be plausibly explained by an overlap of the F 1s Auger decay of core-excited F* in the configuration $1s^1\ 2s^2\ 2p^6$ and core-ionized F$^+$ $1s^1\ 2s^2\ 2p^5$ in the spectrum. That is saying, besides the dissociation channel leading into $CF_3{}^+ + F^*$

discussed above, another channel leading into $CF_3 + F^+$ is also predicted.

The lower and upper (black and red) vertical-bar diagrams in Fig. 9 indicate diagram lines of the F^* and F^+ Auger decays, which are expected based on angular momentum and parity conservation. The energy splittings between the states pertaining to the same final charge (F^+ or F^{2+}) were taken from Ref. [41]. Two offset energies common to all F^+ states and to all F^{2+} states (black bars and red bars), however, were adjusted to give the best fit to the calculated spectrum. Although at the present level our theoretical approach is not sufficient to fully reproduce the expected splittings, or to give accurate intensities, this adjustment reproduces the observed energy positions quite well. It reveals clearly that the three groups of lines in the calculated spectrum are due to the $2s^{-2}$, $2s^{-1}2p^{-1}$ and $2p^{-2}$ Auger transitions. Moreover, the number of lines in each of those groups can be explained by the Auger decays of the two species F^* and F^+. Here we would like to mention that in the theoretical approach we currently take, Auger transition amplitudes are not calculated explicitly, but are estimated based on the projection of population densities on the *a priori* localized core hole. We therefore cannot comment to which extent, additionally to the states discussed above, ICD-like amplitudes resulting in neutral F final states, and a ${CF_3}^{2+}$ fragment, have an influence in the decay. An experimental hint on the importance of those channels is given by the abundance of ${CF_2}^{2+}$ and CF^{2+} (decay products of ${CF_3}^{2+}$), which exceeds the yield of F^{2+} [30].

Our results allow a fresh look to be taken at the two-step model of Auger decay, stating that the Auger decay can be discussed independently from the preceding ionization. For photoelectron energies lower than the Auger kinetic energy, this model is not literally true, as both electrons interact by Coulombic forces once they are in the continuum. This so-called Post Collision Interaction (PCI) leads to an exchange of energy between both electrons that is believed to be understood and will be discounted here. Above PCI, most discussions so far were using the two-step model to address angular correlations between both outgoing electrons. In that sense the two-step model was found to be valid [42], with LVI [3] proving to be the main violating channel.

Here we find that the Auger spectrum strongly depends on the exact amount of energy pumped into the intermediate state. This will not lead to the appearance of interference terms in an LVI-like fashion. Nevertheless, it constitutes a dependence of the Auger spectrum on the primary photoionization step which has not been taken into account in a lot of earlier discussions.

5. Summary

In summary we show that the Auger spectrum of a repulsive core hole state in a molecule is composed of contributions at different conformations that can be distinguished spectroscopically. Using calculations we underpin this interpretation, and show that the nuclear dynamics further enhances these trends. More important in this case however is the effect of zero-point fluctuations already in the neutral ground state. Our observation

shows that Auger spectra can carry a signature of the conformation of the decaying molecule. This might make it possible to extract information about static influences on the conformation of a molecule, e.g. by a solvent shell, as well as on dynamic effects triggered by ionization.

Acknowledgments

Contributions of S. Joshi in early stages of this project are gratefully acknowledged. This work was supported by the Deutsche Forschungsgemeinschaft (HE 3060/5-1), by a Grant-In-Aid for Scientific Research (C) (Contract No. 23540476) of the Ministry of Education, Culture, Sports, Science, and Technology, Japan, the Asahi Glass Foundation and by the Fonds der chemischen Industrie. We thank HZB for the allocation of synchrotron radiation beamtime.

References

[1] Cederbaum L S and Tarantelli F 1993 *J. Chem. Phys.* **99** 5871

[2] Kivilompolo M, Kivimäki A, Aksela H, Huttula M, Aksela S and Fink R F 2000 *J. Chem. Phys.* **113** 662

[3] Püttner R, Hu Y F, Bancroft G M, Aksela H, Nõmmiste E, Karvonen J, Kivimäki A and Aksela S 1999 *Phys. Rev. A* **59**(6) 4438–45

[4] Püttner R, Liu X J, Fukuzawa H, Tanaka T, Hoshino M, Tanaka H, Harries J, Tamenori Y, Carravetta V and Ueda K 2007 *Chem. Phys. Lett.* **445** 6–11

[5] Thürmer S, Oncak M, Ottosson N, Seidel R, Hergenhahn U, Bradforth S E, Slavíček P and Winter B 2013 *Nat. Chem.* **5** 590

[6] Ulrich V, Barth S, Joshi S, Lischke T, Bradshaw A M and Hergenhahn U 2008 *Phys. Rev. Lett.* **100** 143003

[7] Ulrich V, Barth S, Lischke T, Joshi S, Arion T, Mucke M, Förstel M, Bradshaw A M and Hergenhahn U 2011 *J. Electron Spectrosc. Relat. Phenom.* **183** 70–79

[8] Püttner R, Arion T, Förstel M, Lischke T, Mucke M, Sekushin V, Kaindl G, Bradshaw A M and Hergenhahn U 2011 *Phys. Rev. A* **83** 043404 URL `http://link.aps.org/doi/10.1103/PhysRevA.83.043404`

[9] Bolognesi P, O'Keeffe P and Avaldi L 2009 *J. Phys. Chem. A* **113** 15136 URL `http://www.ncbi.nlm.nih.gov/pubmed/20028181`

[10] Iwayama H, Sisourat N, Lablanquie P, Penent F, Palaudoux J, Andric L, Eland J H D, Bucar K, Zitnik M, Velkov Y, Hikosaka Y, Nakano M and Shigemasa E 2013 *J. Chem. Phys.* **138** 024306 ISSN 1089-7690 URL `http://link.aip.org/link/?JCPSA6/138/024306/1`

[11] Griffiths W J, Svensson S, Naves de Brito A, Correia N, Reid C J, Langford M L, Harris F M, Liegener C M and Ågren H 1993 *Chem. Phys.* **173** 109–121

[12] Kivimäki A, Kempgens B, Maier K, Köppe H M, Piancastelli M N, Neeb M and Bradshaw A M 1997 *Phys. Rev. Lett.* **79** 998

[13] Hergenhahn U 2004 *J. Phys. B* **37** R89 URL `http://stacks.iop.org/JPhysB/37/R89`

[14] Goscinski O, Müller J, Poulain E and Siegbahn H 1978 *Chem. Phys. Lett.* **55** 407–412

[15] Falaleyev A G, Andreyev V A and Vovna V I 1992 *Int. J. Quantum Chem.* **43** 573

[16] Moddeman W E 1970 Tech. Rep. ORNL-TM-3012 Oak Ridge National Laboratory

[17] Rye R R and Houston J E 1983 *J. Chem. Phys.* **78** 4321–4330

[18] Gottfried F O, Cederbaum L S and Tarantelli F 1996 *J. Chem. Phys.* **104** 9754–67

[19] Feifel R, Eland J H D, Storchi L and Tarantelli F 2006 *J. Chem. Phys.* **125** 194318

[20] Ueda K, Simon M, Miron C, Leclercq N, Guillemin R, Morin P and Tanaka S 1999 *Phys. Rev. Lett.* **83** 3800

[21] Ueda K, Kitajima M, De Fanis A, Furuta T, Shindo H, Tanaka H, Okada K, Feifel R, Sorensen S L, Yoshida H and Senba Y 2003 *Phys. Rev. Lett.* **90** 233006

[22] Piancastelli M N, Guillemin R, Simon M, Iwayama H and Shigemasa E 2013 *J. Chem. Phys.* **138** 234305 URL `http://www.ncbi.nlm.nih.gov/pubmed/23802958`

[23] Kugeler O, Prümper G, Hentges R, Viefhaus J, Rolles D, Becker U, Marburger S and Hergenhahn U 2004 *Physical Review Letters* **93** 033002

[24] Caprari R S 1995 *Meas. Sci. Technol.* **6** 1063

[25] Lupulescu C, Arion T, Hergenhahn U, Ovsyannikov R, Förstel M, Gavrila G and Eberhardt W 2013 *J. Electron Spectrosc. Relat. Phenom.* **191** 104–11

[26] Gießel T, Bröcker D, Schmidt P and Widdra W 2003 *Rev. Sci. Instrum.* **74** 4620-24

[27] Mitani M, Takahashi O, Saito K and Iwata S 2003 *J. Electron Spectrosc. Relat. Phenom.* **128** 103–117

[28] Takahashi O, Odelius M, Nordlund D, Nilsson A, Bluhm H and Pettersson L G M 2006 *J. Chem. Phys.* **124** 064307–9

[29] Schimmelpfennig B, Nestmann B and Peyerimhoff S 1995 *J. Electron Spectrosc. Relat. Phenom.*

74 173 – 186
[30] Guillemin R, Stolte W C, Piancastelli M N and Lindle D W 2010 *Phys. Rev. A* **82**(4) 043427
[31] Itchkawitz B S, Kempgens B, Köppe H M, Feldhaus J, Bradshaw A M and Peatman W B 1995 *Rev. Sci. Instrum.* **66** 1531-1533
[32] Kempgens B, Itchkawitz B S, Erlebach W, Köppe H M, Feldhaus J and Bradshaw A M Absolute photoabsorption cross section measurements of atoms and molecules in the K-edge energy range, unpublished
[33] LaVilla R E 1973 *J. Chem. Phys.* **58** 3841–3848
[34] Saito N, Bozek J D and Suzuki I H 1994 *Chem. Phys.* **188** 367379
[35] Barth S, Oncak M, Ulrich V, Mucke M, Lischke T, Slavicek P and Hergenhahn U 2009 *J. Phys. Chem. A* **113** 13519
[36] Menzel A, Langer B, Viefhaus J, Whitfield S B and Becker U 1996 *Chem. Phys. Lett.* **258** 265
[37] Björneholm O, Sundin S, Svensson S, Marinho R R T, Naves de Brito A, Gel'mukhanov F and Ågren H 1997 *Phys. Rev. Lett.* **79**(17) 3150–3153
[38] Hergenhahn U 2011 *J. Electron Spectrosc. Relat. Phenom.* **184** 78
[39] Buth C, Santra R and Cederbaum L S 2003 *J. Chem. Phys.* **119** 10575
[40] Thomas T D, Miron C, Wiesner K, Morin P, Carroll T X and Sæthre L J 2002 *Phys. Rev. Lett.* **89** 223001
[41] NIST Atomic Spectra Database, Version 5, http://www.nist.gov/pml/data/asd.cfm
[42] Weber T, Weckenbrock M, Balser M, Schmidt L, Jagutzki O, Arnold W, Hohn O, Schöffler M, Arenholz E, Young T, Osipov T, Foucar L, De Fanis A, Díez Muiño R, Schmidt-Böcking H, Cocke C L, Prior M H and Dörner R 2003 *Phys. Rev. Lett.* **90** 153003

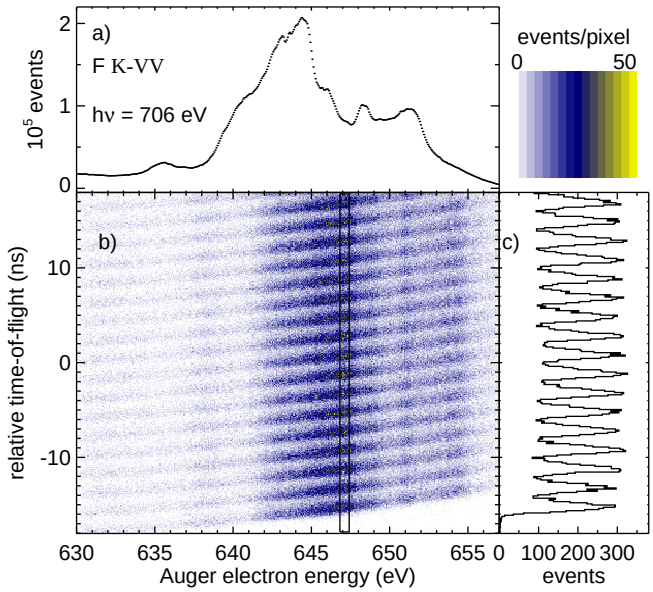

Figure 1. (color online) a) Non-coincident CF_4 F K-VV Auger spectrum recorded with 706 eV photons. b) Auger time-of-flight (t_{au}) vs. Auger energy (ε_{au}) relation for some non-coincident F K-VV Auger electrons. The number of events per pixel is shown on a linear colour scale. c) Summation of the events in the marked rectangle along the Auger energy axis.

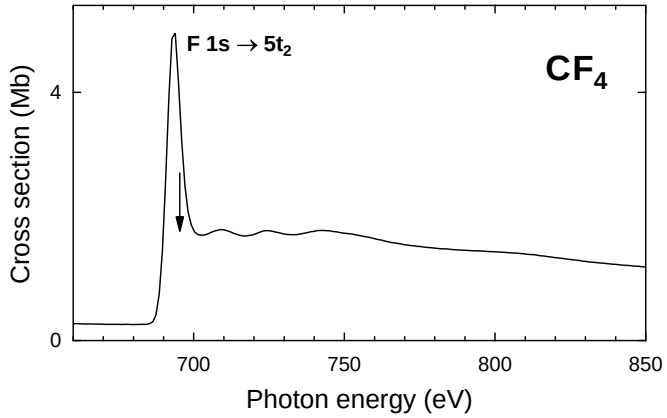

Figure 2. The photoabsorption spectrum of CF_4 at the fluorine K-edge [32]. The energy scale aligns with Ref. [34]. An arrow marks the vertical ionization energy.

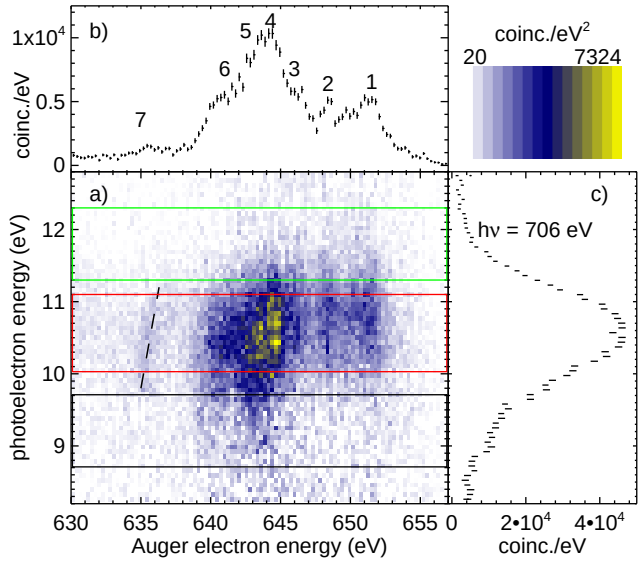

Figure 3. (color online) a) Dependence of the F K-VV Auger spectra of CF_4 on the photoelectron kinetic energy. For every Auger energy ε_{au} (horizontal axis) contributions of all photoelectron energies ε_{ph} (vertical axis), recorded as e^-, e^- coincidences, are shown on a linear color scale in units of coincident events per eV^2. Panels b) and c): Summations over all photoelectron energies and all Auger electron energies, respectively. These correspond to the conventional (non-coincident) photoelectron and Auger spectra. The labelling in panel b) is according to [11]. Rectangles in panel a) designate the regions that will be compared in figure 4. The dashed line is discussed in the text.

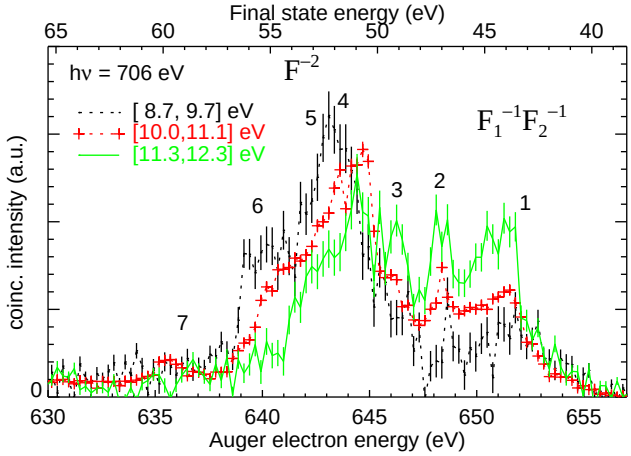

Figure 4. (color online) F K-VV Auger spectra of CF_4 for photoelectrons within three different kinetic energy intervals (ε_{ph}, see figure label). Spectra were normalized to equal total area. Lines are drawn to guide the eye. The trace designated by '+' symbols and a dotted line corresponds to the central region of the photoelectron spectrum (vertical excitation). The trace shown by a solid line pertains to photoelectrons on the high kinetic energy side of the vertical peak, the third trace to photoelectrons on the low kinetic energy side. In the same order, the traces shown here correspond to the middle, top and bottom rectangular regions in panel a) of figure 3. The final state energy has been calculated as $E_b - \varepsilon_{au}$.

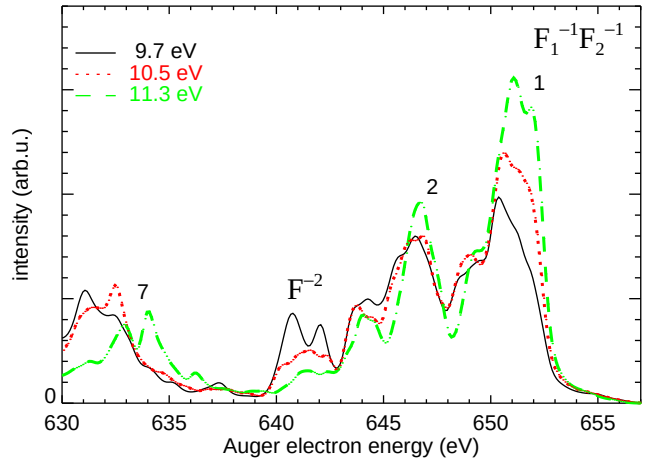

Figure 5. (color online) F K-VV Auger spectra of CF_4 calculated for photoelectrons at different ionization energy. The calculated vertical binding energy has been adjusted to the experimental value of E_b [11]. Ionization energies have been converted to kinetic energies (see figure label) using $h\nu = 706$ eV. Labels $F_1^{-1}F_2^{-1}$ and F^{-2} designate the dominant electronic character of the respective final states, as discussed in the text. Numerical labels refer to figure 4.

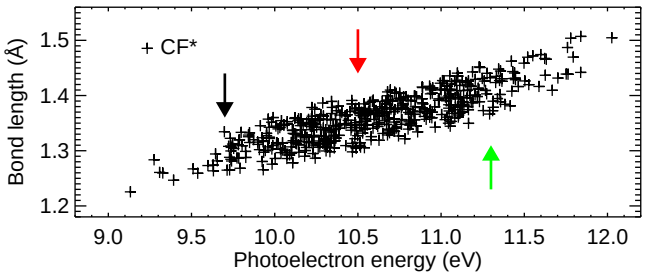

Figure 6. (color online) C-F* bondlengths from a sample of 500 molecular dynamics snapshots of the CF_4 core ionized state, vs. photoelectron energy ε_{ph}. Arrows mark the energies shown in figure 5.

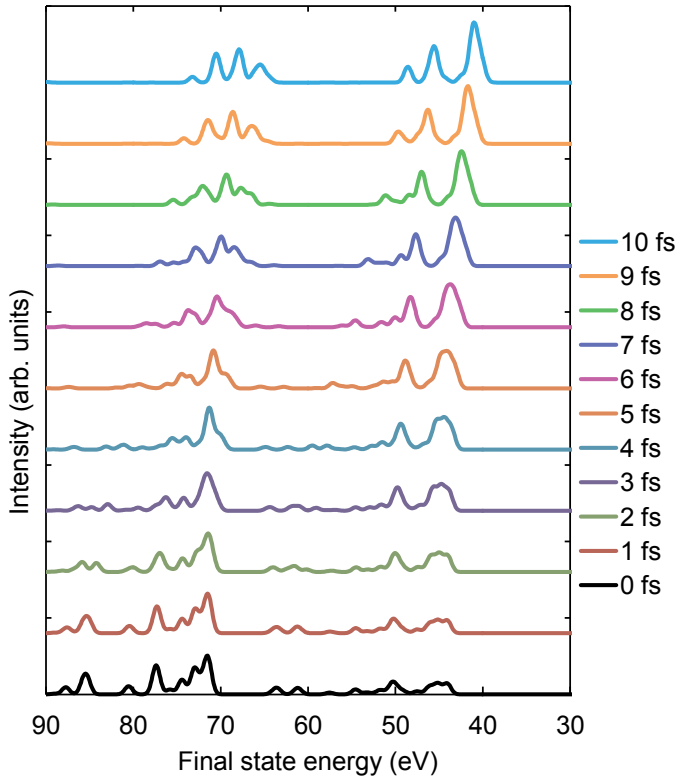

Figure 7. (color online) Calculated temporal evolution of the CF_4 F K-VV Auger spectrum, for a molecule at the ground state equilibrium geometry. All traces are normalized to the same overall Auger intensity.

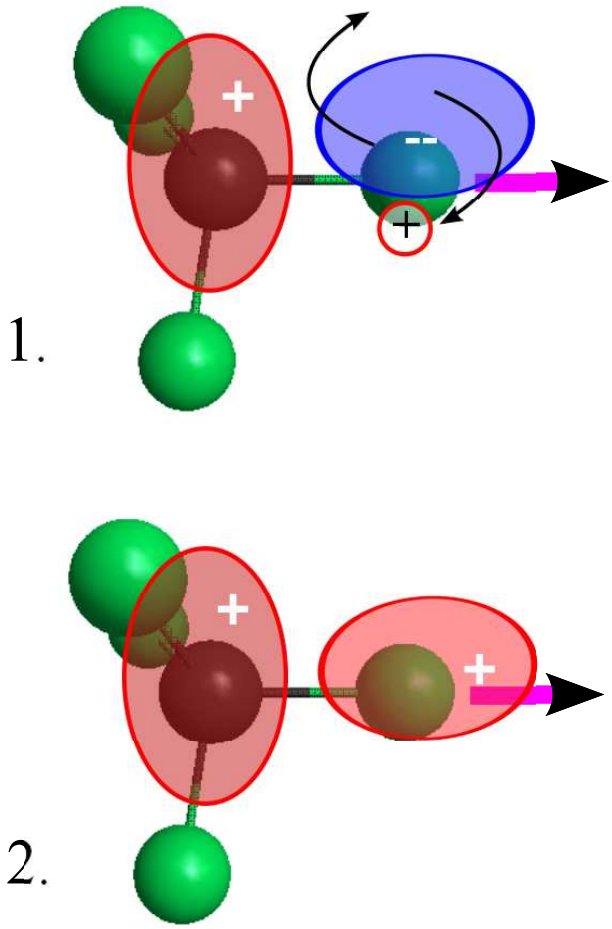

Figure 8. (color online) Simplified sketch of the mechanism which leads to the preferential population of $F_1^{-1}F_2^{-1}$ states from CF_4 molecules with an elongated C-F* bond. In the core ionized state, the molecule has a tendency to dissociate into an F* atom, which nevertheless caries the core hole (right-hand side), and a CF_3^+ fragment. 1. Before Auger decay, the single atom is neutralized by an excess charge taken from the delocalized charge cloud of the remainder of the molecule. 2. After Auger decay has taken place in an atomic-like fashion, the core hole on the right hand side is filled, and another electron is missing e.g. from a lone pair orbital on the F atom concerned. Not shown: Alternatively, the core hole may decay in an ICD like fashion, creating a second vacancy on the CF_3 fragment.

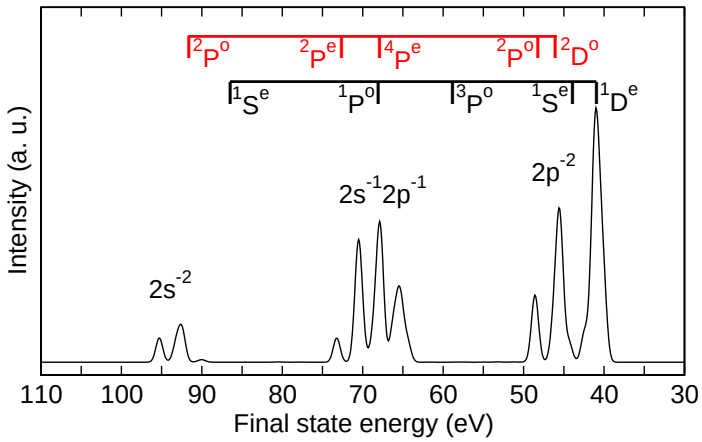

Figure 9. (color online) The full calculated Auger spectrum for decays occuring 10 fs after the photoionization process. The higher (black) and the lower (red) vertical-bar diagrams indicate the relative energy positions of expected diagram lines of the F 1*s* decays of F^* and F^+, respectively. See text for details.